

Durham Research Online

Deposited in DRO:

07 April 2015

Version of attached file:

Accepted Version

Peer-review status of attached file:

Peer-reviewed

Citation for published item:

Hilton, R. G. and Galy, A. and Hovius, N. and Chen, M.-C. and Horng, M.-J. and Chen, H. (2008)
'Tropical-cyclone-driven erosion of the terrestrial biosphere from mountains.', *Nature geoscience.*, 1 (11). pp. 759-762.

Further information on publisher's website:

<http://dx.doi.org/10.1038/ngeo333>

Publisher's copyright statement:**Additional information:**

Use policy

The full-text may be used and/or reproduced, and given to third parties in any format or medium, without prior permission or charge, for personal research or study, educational, or not-for-profit purposes provided that:

- a full bibliographic reference is made to the original source
- a [link](#) is made to the metadata record in DRO
- the full-text is not changed in any way

The full-text must not be sold in any format or medium without the formal permission of the copyright holders.

Please consult the [full DRO policy](#) for further details.

1 **Tropical-cyclone-driven erosion of the terrestrial biosphere from**
2 **mountains**

3 Robert. G. Hilton, Albert Galy, Niels Hovius

4 Department of Earth Sciences, University of Cambridge, Downing Street, Cambridge, CB2 3EQ, UK

5 Meng-Chiang Chen

6 Taroko National Park Headquarters, Fu-Su Village, Hualien, 972, Taiwan

7 Ming-Jame Horng

8 Water Resources Agency, Ministry of Economic Affairs, Taipei, Taiwan

9 Hongey Chen

10 Department of Geoscience, National Taiwan University, Taipei, Taiwan

11

12 **The transfer of organic carbon from the terrestrial biosphere to the oceans via**
13 **erosion and riverine transport constitutes an important component of the global**
14 **carbon cycle¹⁻⁴. More than one third of this organic carbon flux comes from**
15 **sediment-laden rivers that drain the mountains in the western Pacific region^{3,5}. This**
16 **region is prone to tropical cyclones, but their role in sourcing and transferring**
17 **vegetation and soil is not well constrained. Here we measure particulate organic**
18 **carbon load and composition in the LiWu River, Taiwan, during cyclone-triggered**
19 **floods. We correct for fossil particulate organic carbon using radiocarbon, and find**
20 **that the concentration of particulate organic carbon from vegetation and soils is**
21 **positively correlated with water discharge. Floods have been shown to carry large**
22 **amounts of clastic sediment⁶. Non-fossil particulate organic carbon transported at**
23 **the same time may be buried offshore under high rates of sediment accumulation⁷⁻⁹.**
24 **We estimate that on decadal timescales, 77–92% of non-fossil particulate organic**
25 **carbon eroded from the LiWu catchment is transported during large, cyclone-**
26 **induced floods. We suggest that tropical cyclones, which affect many forested**
27 **mountains within the Intertropical Convergence Zone¹⁰, may provide optimum**
28 **conditions for the delivery and burial of non-fossil particulate organic carbon in the**
29 **ocean. This carbon transfer is moderated by the frequency, intensity and duration**
30 **of tropical cyclones.**

31 Mountain rivers carry a mix of clastic sediment and POC, mobilised by hillslope
32 mass wasting at a rate proportional to the tectonic advection of rock mass in mountain
33 belts^[11,12]. The riverine POC is derived from vegetation, soil, and bedrock^[13]. Erosion and
34 burial of photosynthetically-derived organic carbon is a sink of atmospheric CO₂^[4,14],
35 reburial of fossil POC from sedimentary rocks^[15] is not. It is therefore important to
36 quantify the proportions of fossil and non-fossil POC in the river load, and the conditions
37 of transfer which determine the likelihood of its burial. We have done this in a mountain
38 river in Taiwan.

39 In Taiwan, as elsewhere in the west Pacific rim, intense precipitation, combined
40 with high tectonic rates drive rapid mass wasting and fluvial sediment transfer^[16]. These
41 conditions promote rapid growth and erosional overturning of hillslope vegetation^[17], and
42 the delivery of soil and biomass to river channels. Erosion and sediment transfer peak
43 during storm floods. Across the west Pacific there is a strong gradient in cyclonic storm
44 activity, and Taiwan has a high tropical cyclone (typhoon) hit rate, about 3 per year^[18].
45 There, we have focused on the LiWu River. Set entirely within a national park, it drains
46 435 km² of the densely forested (up to ~3000 m asl) Taiwan Central Range to the Pacific
47 Ocean. Storage of sediment in its bedrock channel is limited and decadal sediment yields
48 are known from river gauging^[16].

49 To determine the quantity and source of POC in the LiWu River we have
50 measured the organic carbon concentration (C_{org}) and ¹⁴C of suspended load (Methods).
51 ¹⁴C helps define the proportion of non-fossil POC, since fossil POC from bedrock
52 contains only a trace of ¹⁴C. Suspended load samples were collected at water discharges
53 (Q_w) of 1.1 to 12 times the 30 year mean (Q_{mean}=33 m³ s⁻¹) (Figure 1 and Supplementary
54 Table 1). In these samples C_{org} ranged from 0.16% to 0.42% and the fraction modern
55 (from ¹⁴C, Methods), F_{mod}, from 0.04 to 0.43 (Supplementary Table 1). Soils in the
56 Taiwan mountains contain up to 10 times more organic carbon than suspended load
57 samples with an average F_{mod}~1 (Supplementary Table 2). F_{mod} is likely ~1.1 in live
58 vegetation (Methods). The low C_{org} and F_{mod} of riverine POC therefore reflect the
59 dominance of clastic sediment supply by landslides, mobilising the rocky substrate and
60 mixing non-fossil POC with large quantities of fossil POC from bedrock, as in other
61 mountain belts around the Pacific^[12,13].

62 We find that non-fossil POC concentration in the suspended load (POC_{mod} , the
63 concentration of POC derived from vegetation and soil, in mg L^{-1}) was positively
64 correlated with Q_w and there was no dilution at high Q_w (Figures 1 and 2). Such
65 relationships are commonly invoked for clastic sediment transfer^[19,20,21] where a power
66 law relates suspended sediment concentration (SSC, mg L^{-1}) to Q_w , with variability in
67 scaling reflecting the supply of clastic sediment. The non-linear increase in POC_{mod} with
68 Q_w (Figure 2) implies a strong link between climate and the erosion of the terrestrial
69 biosphere in this river catchment.

70 To assess whether this relationship may be a common feature of mountain rivers
71 in forested topography, it is necessary to first consider the processes responsible for
72 mobilising soil and vegetation from hillslopes. It is commonly thought that surface runoff
73 (overland flow) delivers organic-rich particles from banks and soils to the river during
74 moderate precipitation^[22], and that rocky landslide debris dilutes non-fossil POC at high
75 Q_w and SSC^[13,23]. In a sample collected from the LiWu River at 1.1 times Q_{mean} , shortly
76 after 22 mm of rain in 30 hours, $F_{\text{mod}} = 0.41$ (Supplementary Table 1), supporting this
77 notion. However, samples taken at flood peaks during typhoons Mindulle (July 2004) and
78 Aere (August 2004) had elevated POC concentrations, associated with an increase in F_{mod}
79 and concentration of non-fossil POC (POC_{mod} , mg L^{-1}) in the suspended load (Figure 1).
80 At the peak of the Mindulle flood 43% of suspended POC was derived from vegetation
81 and soil. At that time intense precipitation (Figure 1) probably resulted in widespread
82 transport of materials by overland flow^[22], while landslides affected $\sim 0.05\%$ of the
83 catchment area (Methods). Both mechanisms harvested photosynthetic organic carbon
84 ranging from soil litter to tree trunks. Mechanical breakdown of this material during
85 transport to typical suspended sediment grain size likely added to the observed increase in
86 F_{mod} and POC_{mod} at the typhoon peak.

87 Samples collected after at least several hours of sustained rainfall show a positive
88 non-linear relation between Q_w and POC_{mod} described by a power law (Figure 2).
89 Samples collected during dry intervals also show a positive relationship but follow a
90 power law with a lower exponent. Without rain, the principle source of non-fossil POC is
91 river sediment in channels^[12] containing mainly bedrock clasts. Moderate rainfall causes
92 overland flow on hillslopes, washing soil and organic litter into the channel which

93 increases POC_{mod} . During extreme rainfall, landsliding adds both photosynthetic and
94 fossil carbon to this runoff flux. Overall, the effect of rainfall appears to be an increase in
95 POC_{mod} for a given discharge by up to a factor five (Figure 2). Given the common nature
96 of the erosion processes outlined here^[12,13,22] this climatic control on POC_{mod} could be a
97 general effect in humid mountain belts, influencing non-fossil POC yields.

98 Using the observed scaling of Q_w , POC concentration and POC_{mod} , we estimate
99 that the total suspended POC in the Mindulle flood was ~14,200 tC, of which ~5500 tC
100 came from non-fossil sources (Methods). The non-fossil flux represents a carbon yield of
101 13 tC km^{-2} , in a storm with a return time of 1/2 year. The total amount of organic carbon
102 (soils and standing biomass) residing on Taiwan mountain slopes is $\sim 25 \times 10^3 \text{ tC km}^{-2}$
103 ^[18,24]. Typhoon Mindulle therefore removed ~0.05% of the hillslope carbon store. This is
104 similar to the proportion of the catchment disrupted by landslides (Methods) confirming
105 that material delivered by mass wasting is an important source of suspended load non-
106 fossil POC^[12,13].

107 We assume that the two Q_w - POC_{mod} relationships in Figure 2 bound a likely range
108 of POC_{mod} for a given Q_w , and combined them with the record of Q_w since 1970. This
109 gives an average yield of non-fossil POC of 16 to 202 $\text{tC km}^{-2} \text{ yr}^{-1}$ for the LiWu
110 catchment (Methods). Most of the uncertainty derives from the extrapolation to very high
111 Q_w where no direct measurements of POC_{mod} are available. This estimate does not
112 include coarse non-fossil POC which may float or travel in the bed load. Even so, this
113 erosional flux of non-fossil POC is easily sustained by the present net primary
114 productivity of the terrestrial biosphere^[25].

115 The POC yield from the LiWu River is amongst the highest recorded globally^[4,23].
116 Many small rivers in the Intertropical Convergence Zone (ITCZ) have high total POC
117 yields^[3,4], and 50 to 90 MtC yr^{-1} is thought to enter the oceans from islands of the west
118 Pacific alone^[5]. The corresponding average specific total POC yield is $\sim 10\text{-}20 \text{ tC km}^{-2} \text{ yr}^{-1}$,
119 but this is not entirely comprised of recent atmospheric CO_2 and likely contains a
120 fraction of fossil POC from bedrocks^[15]. In mountain catchments outside the ITCZ where
121 F_{mod} measurement allow quantification (US rivers: Siuslaw, Noyo, Navarro and Eel),
122 non-fossil POC yields are $\sim 5\text{-}8 \text{ tC km}^{-2} \text{ yr}^{-1}$ ^[13]. The LiWu and other upland rivers

123 affected by large tropical storms, for example on North Island New Zealand^[13], have non-
124 fossil POC yields of 2-10 times greater.

125 Ultimately it is the burial of this atmospherically-derived POC in sediments that
126 matters for long-term C cycling^[4,14]. More than 90% of non-fossil POC is thought to be
127 remineralised after entering the ocean^[26]. However, floods from mountain catchments can
128 have very high SSC^[19] and large sediment loads (Figure 3), increasing offshore
129 deposition rates and the burial efficiency of organic matter^[7,8,9]. Importantly, many
130 Taiwanese rivers deliver clastic sediment to the ocean at hyperpycnal SSC during
131 typhoon floods^[6,21]. Hyperpycnal river plumes can trigger turbidity currents that bypass
132 shallow marine depocentres^[19], transfer non-fossil POC direct to deep ocean basins and
133 deposit thick sediment beds in which POC preservation is maximal. During the Mindulle
134 flood, about 90% of the non-fossil POC was transported during 14 hours when the LiWu
135 River had a hyperpycnal density (Methods). Extrapolating using measured POC_{mod} and
136 Q_w (Figure 2), we estimate that since 1970, 77-92% of all non-fossil POC was
137 transported in floods with a return time greater than 1/2 year and likely hyperpycnal SSC
138 (Figure 3, Methods). In Taiwan such floods, during which the burial potential of non-
139 fossil POC is maximal, occur almost exclusively during tropical cyclones.

140 Many mountain rivers are capable of reaching hyperpycnal concentrations. These
141 turbid flows are influenced by a number of factors apart from large storms including
142 earthquakes and bedrock lithology^[20,21]. While lithology sets the sensitivity of a
143 catchment to external triggers of erosion, earthquakes and associated hyperpycnal flows
144 typically recur on timescales of centuries, even in orogens with very high rates of rock
145 uplift and erosion^[19]. In contrast, storms of varying magnitude occur on decadal or
146 shorter timescales. The forested mountain belts of the ITCZ have an optimal combination
147 of tectonic activity, driving rapid erosion, and frequent tropical cyclones^[10] which cause
148 floods that harvest modern organic carbon and clastic sediment and optimise the
149 likelihood of burial. Outside the ITCZ non-fossil POC yields may be high, such as in
150 New Zealand^[12,13], but in the absence of frequent tropical cyclones only a limited fraction
151 of this atmospheric CO₂ may be delivered by sediment-laden river plumes to the ocean.
152 Tropical cyclones deliver heavy rainfall, driving the erosion of terrestrial biomass from
153 slopes by common runoff and mass wasting processes^[12,13,23]. This results in a positive

154 relationship between POC_{mod} and Q_w in the river suspended load (Figure 2). Individual
155 floods contribute to the erosion of non-fossil POC according to their return time, and in a
156 catchment affected by tropical cyclones, the largest floods dominate in the long-term
157 (Figure 3). These floods, occurring every $\sim 1-10$ years, have the highest density and
158 greatest sediment loads, and are therefore also most likely to cause the geological burial
159 of POC.

160 This mechanism explains the abundance of terrestrial POC in modern^[27] and
161 Cenozoic turbidites^[28] within the ITCZ, and affects the total drawdown of atmospheric
162 CO_2 through erosion of the terrestrial biosphere. Due to its dependence on floods (Figure
163 3), this carbon sequestration mechanism is sensitive to changes in the frequency of the
164 most intense tropical cyclones. Such changes, which have been linked to the climate state
165 of the ocean and atmosphere^[10,29,30], have the potential to impact regional and global
166 transfers of photosynthetic organic carbon from the terrestrial biosphere to the deep
167 ocean. Increasing sea surface temperatures may increase the intensity of cyclones^[30] and
168 therefore enhance the transfer and storage of terrestrial biogenic POC in ocean sediments.
169 Depending on the exact link to atmospheric CO_2 , this may give rise to a negative carbon-
170 cycle feedback on cyclone climate.

171

172 **Methods Summary**

173 **Sampling and geochemistry of POC.** Samples of suspended sediment were collected at
174 Lushui station and filtered and dried on site. Water discharge and precipitation are
175 measured automatically, at Lushui and within the catchment respectively. Soil samples
176 were collected from uncultivated surface horizons across the Taiwan Central Range.
177 After drying and homogenisation by grinding, sediments were leached with HCl to
178 remove carbonate. Organic carbon concentrations were determined by elemental
179 analyser-isotope ratio mass spectrometer (EA-IRMS) on a Costech-EA coupled via
180 CONFLO-III to a MAT-253 IRMS^[12]. An accelerator mass spectrometer (AMS) at
181 NERC Radiocarbon laboratory, East Kilbride (Allocation numbers 1203.1006 and
182 1228.0407) was used to measure ^{14}C . Blanks of torched sand subjected to this procedure
183 returned negligible concentrations of C. Organic ^{14}C standards subjected to carbonate
184 removal returned F_{mod} within 1σ of consensus values.

185 **Non-fossil POC and suspended sediment transfer.** The co-variation of POC_{mod} and Q_w
186 is described by a power law. Within the whole data set two different trends are
187 recognised (Figure 2). Samples collected during rainfall episodes are closely fit by the
188 power law $POC_{mod}=0.01*Q_w^{1.59}$ ($R^2=0.99$, $\chi^2=1.8$). All other samples have lower POC_{mod}
189 at a given Q_w and are well described by a second power law ($POC_{mod}=0.02*Q_w^{1.11}$;
190 $R^2=0.96$, $\chi^2=0.27$). These power laws were used as upper and lower bounds in predicting
191 POC_{mod} for each day of the gauged record (1970-1999, 2003-2004). Suspended sediment
192 rating curves based on our measurements and the full gauging record were used in a
193 similar manner to investigate suspended sediment transfer.

194 **Storm-triggered landslide mapping.** Landslides were mapped by differencing
195 LandsatTM satellite imagery acquired before and after typhoon Mindulle (18/06/2004,
196 20/07/2004) using ArcGIS software. Resolution is $\sim 90m \times 90m$. Mapped scars disrupt
197 $0.23km^2$ of the catchment.

198

199 **References**

- 200 1. Ittekkot, V. Global trends in the nature of organic-matter in river suspensions. *Nature*
201 **332**, 436–438 (1988).
- 202 2. Meybeck, M. C, N, P, and S in rivers, From sources to global inputs. In *Interactions of*
203 *C, N, P and S Biogeochemical Cycles and Global Change*, 163–193 (Berlin, Springer-
204 Verlag, 1993).
- 205 3. Schlünz, B. & Schneider, R. R. Transport of terrestrial organic carbon to the oceans by
206 rivers: re-estimating flux and burial rates. *Int. J. Earth Sci.* **88**, 599–606 (2000).
- 207 4. Stallard, R. F. Terrestrial sedimentation and the carbon cycle: Coupling weathering and
208 erosion to carbon burial. *Glob. Biogeochem. Cycles* **12**, 231–257 (1998).
- 209 5. Lyons, W. B., Nezat, C. A., Carey, A. E. & Hicks, D. M. Organic carbon fluxes to the
210 ocean from high-standing islands. *Geology* **30**, 443–446 (2002).
- 211 6. Milliman, J. D. & Kao, S. J. Hyperpycnal discharge of fluvial sediment to the ocean:
212 Impact of Super-Typhoon Herb (1996) on Taiwanese rivers. *J. Geol.* **113**, 503–516
213 (2005).
- 214 7. Canfield, D. E. Factors influencing organic-carbon preservation in marine sediments.
215 *Chem. Geol.* **114**, 315–329 (1994).

- 216 8. Burdige, D. J. Burial of terrestrial organic matter in marine sediments: A reassessment.
217 *Glob. Biogeochem. Cycles* **19**, GB4011 (2005).
- 218 9. Galy, V. *et al.* Efficient organic carbon burial in the Bengal fan sustained by the
219 Himalayan erosional system. *Nature* **450**, 407–410 (2007).
- 220 10. Webster, P. J., Holland, G. J., Curry, J. A. & Chang, H. R. Changes in tropical
221 cyclone number, duration, and intensity in a warming environment. *Science* **309**, 1844–
222 1846 (2005).
- 223 11. Burbank, D. W. *et al.* Bedrock incision, rock uplift, and threshold hillslopes in the
224 northwestern Himalaya. *Nature* **379**, 505–510 (1996).
- 225 12. Hilton, R. G., Galy, A. & Hovius, N. Riverine particulate organic carbon from an
226 active mountain belt: The importance of landslides. *Glob. Biogeochem. Cycles* **22**,
227 GB1017 (2008).
- 228 13. Leithold, E. L., Blair, N. E. & Perkey, D. W. Geomorphologic controls on the age of
229 particulate organic carbon from small mountainous and upland rivers. *Glob. Biogeochem.*
230 *Cycles* **20**, GB3022 (2006).
- 231 14. Hayes, J. M., Strauss, H. & Kaufman, A. J. The abundance of ^{13}C in marine organic
232 matter and isotopic fractionation in the global biogeochemical cycle of carbon during the
233 past 800 Ma. *Chem. Geol.* **161**, 103–125 (1999).
- 234 15. Blair, N. E. *et al.* The persistence of memory: The fate of ancient sedimentary organic
235 carbon in a modern sedimentary system. *Geochim. Cosmochim. Acta* **67**, 63–73 (2003).
- 236 16. Dadson, S. J. *et al.* Links between erosion, runoff variability and seismicity in the
237 Taiwan orogen. *Nature* **426**, 648–651 (2003).
- 238 17. Lin, K. C., Duh, C. T., Ma, F. C. & Wang, H. H. Biomass and nutrient content of
239 woody debris in the Fu-shan subtropical broadleaf forest of northeastern Taiwan. *Taiwan*
240 *J. For. Sci.* **18**, 235–244 (2003).
- 241 18. Wu, C. C. & Kuo, Y. H. Typhoons affecting Taiwan: Current understanding and
242 future challenges. *Bull. Am. Meteorol. Soc.* **80**, 67–80 (1999).
- 243 19. Mulder, T. & Syvitski, J. P. M. Turbidity currents generated at river mouths during
244 exceptional discharges to the world oceans. *J. Geol.* **103**, 285–299 (1995).

- 245 20. Hicks, D. M., Gomez, B. & Trustrum N. A. Event suspended sediment characteristics
246 and the generation of hyperpycnal plumes at river mouths: East coast continental margin,
247 North Island, New Zealand, *J. Geol.* **112**, 471–485 (2004).
- 248 21. Dadson, S. et al. Hyperpycnal river flows from an active mountain belt. *J. Geophys.*
249 *Res.* **110**, F04016 (2005).
- 250 22. Larsen, M. C., Torres-Sanchez, A. J. & Concepcion I. M. Slopewash, surface runoff
251 and fine litter transport in forest and landslide scars in humid tropical steeplands,
252 Luquillo experimental forest, Puerto Rico. *Earth Surf. Proc. Land.* **24**, 481–502 (1999).
- 253 23. Ludwig, W., Probst, J. L. & Kempe, S. Predicting the oceanic input of organic carbon
254 by continental erosion. *Glob. Biogeochem. Cycles* **10**, 23–41 (1996).
- 255 24. Chang, Y. F., Lin, S. T. & Tsai, C. C. Estimation of soil organic carbon storage in a
256 Cryptomeria plantation forest of northeastern Taiwan. *Taiwan J. For. Sci.* **21**, 383–393
257 (2006).
- 258 25. Zaks, D. P. M., Ramankutty, N., Barford, C. C. & Foley, J. A. From Miami to
259 Madison: Investigating the relationship between climate and terrestrial net primary
260 production. *Glob. Biogeochem. Cycles* **21**, GB3004 (2007).
- 261 26. Hedges, J. I., Keil, R. G. & Benner, R. What happens to terrestrial organic matter in
262 the ocean? *Org. Geochem.* **27**, 195–212 (1997).
- 263 27. Nakajima, T. Hyperpycnites deposited 700 km away from river mouths in the central
264 Japan Sea. *J. Sediment. Res.* **76**, 60–73 (2006).
- 265 28. Saller, A., Lin, R. & Dunham, J. Leaves in turbidite sands: The main source of oil and
266 gas in the deep-water Kutei Basin, Indonesia. *AAPG Bull.* **90**, 1585–1608 (2006).
- 267 29. Emanuel, K. Increasing destructiveness of tropical cyclones over the past 30 years.
268 *Nature* **436**, 686–688 (2005).
- 269 30. Elsner, J. B., Kossin, J. P. & Jagger, T. H. The increasing intensity of the strongest
270 tropical cyclones. *Nature* **455**, 92–95 (2008).

271

272 **Supplementary Information** is linked to the online version of the paper at
273 www.nature.com/nature.

274

275 **Acknowledgements** This work was supported by the UK Natural Environmental
276 Research Council (NERC) and The Cambridge Trusts. Radiocarbon analysis were carried
277 out on NERC allocation numbers 1203.1006 and 1228.0407. We thank Taroko National
278 Park for access to research sites.

279 **Author Contributions** R.G.H., A.G. and N.H. wrote the manuscript. M.C.C. collected
280 the suspended load samples and R.G.H. and A.G collected soil samples. M.J.H. and H.C.
281 provided hydrological data.

282 **Competing interests statement** The authors declare that they have no competing
283 financial interests.

284 **Correspondence** and request for materials should be addressed to R. G. H.
285 (rgh31@esc.cam.ac.uk)

286

287 **Figure Captions**

288 **Figure 1: Source and concentration of riverine particulate organic carbon (POC)**
289 **during typhoon floods in 2004.** Frequent sampling of suspended load from the LiWu
290 River, Taiwan in Julian Day time, with hourly water discharge (Q_w , $m^3 s^{-1}$) during
291 typhoons Mindulle and Aere (light grey) and precipitation (ppt, in $mm hr^{-1}$ multiplied by
292 a constant factor 10) in dark grey. Note the difference in time increments between flood
293 events. Grey diamonds show total particulate organic carbon concentration (POC_{tot} , mg
294 L^{-1}). Non-fossil POC concentrations (POC_{mod} , $mg L^{-1}$, black circles) were calculated from
295 F_{mod} (text) where stars indicate samples labeled in Figure 2. Both floods had high POC
296 near peak discharge, caused by increased F_{mod} and POC_{mod} .

297

298 **Figure 2: Positive, non-linear relationships between non-fossil POC concentration**
299 **(POC_{mod} , $mg L^{-1}$) and water discharge (Q_w , $m^3 s^{-1}$).** Dashed line is power law best fit
300 through samples collected after sustained rainfall near the peak of typhoon-induced
301 floods (shown with white stars, see also Figure 1) and outside the typhoon season
302 (indicated by white triangle). $R^2=0.99$, $\chi^2=1.8$. Dotted line is power law best fit through
303 the remaining data ($R^2=0.96$, $\chi^2=0.3$). For the available data these fits delimit a range of
304 possible POC_{mod} for a given Q_w . The positive non-linear trend highlights an important
305 role of climate to the POC_{mod} and it's transfer.

306

307 **Figure 3: Cumulative discharge, suspended sediment and non-fossil POC transfer**

308 **versus return time of a given flow.** $RT_i=(T+1)/N_i$ where RT_i is return time (yr) of the i th

309 observation, T the length of the record (32 years), and N_i is rank of i th observation, daily

310 water discharge (Q_w), suspended sediment (SS) and non-fossil POC (POC_{nf}) transfer

311 ranked in descending order with maximum at $N=1$. POC_{nf} transfer is calculated from Q_w

312 with the models describing range of data (Figure 2). Dashed and dotted lines show mean

313 Q_w and typhoon Mindulle flood (0.5 yr) RT, respectively. Floods dominate the erosion of

314 POC from the terrestrial biosphere, with flows with $RT>0.5$ yr responsible for 77-92% of

315 the total transfer.

316

317 **Methods**

318 **Sampling.** Suspended sediment samples were collected at the Lushui gauging station,
319 LiWu River (24.1667°N, 121.5052°E), where water discharge (Q_w) is recorded by the
320 Water Resources Agency (<http://gweb.wra.gov.tw>, Site 2460H005)^[31] and precipitation
321 by the Central Weather Bureau at La-Shao upstream of the gauging station (C1T800,
322 24.2064°N, 121.4458°E). For each sample 250 ml of turbid water were collected from the
323 surface of the main channel where turbulence was evident, in a wide-mouthed plastic
324 bottle thoroughly rinsed with river water. This assumes negligible difference in POC
325 concentration in suspended load within the turbulent channel^[32]. Samples were filtered
326 through 0.2 μm nylon membrane filters checked for damage after filtration to avoid
327 sample contamination. Each sample was dried at 80°C, weighed to determine suspended
328 sediment concentration (SSC, mg L^{-1}) and stored in sealed glass dishes. Blanks (n=3) of
329 torched sand was subjected to the same procedure. Approximately 500 cm^3 of bulk soil
330 were sampled from surface horizons (A-E) from uncultivated areas across Taiwan Central
331 Range (n=10).

332

333 **Geochemistry.** River load and blank were homogenised by grinding in an agate mill.
334 Soils were homogenised using a mill grinder. The ground mass was acidified with 5M
335 HCl and heated to 80°C for 4 hours to remove detrital carbonate^[12]. A similar procedure
336 was performed on two ^{14}C standards (IAEA-C5; TIRI-Barleymash) to quantify bias
337 introduced by this carbonate removal on organic matter. Concentrations of organic
338 carbon (C_{org}) were determined by combustion at 1020°C in a Costech elemental analyser
339 coupled via a CONFLO III to a MAT 253 stable isotope ratio mass spectrometer.
340 Analysis of the blank returned negligible concentrations of carbon (0.93 μg), representing
341 1.7% of the typical amount of C in each sample aliquot. ^{14}C was measured by AMS after
342 graphitisation of samples at NERC Radiocarbon laboratory, East Kilbride. ^{14}C standards
343 subjected to the carbonate removal procedure returned ^{14}C within 1 σ of consensus values.
344 The fraction of modern ^{14}C (fraction modern, F_{mod}) is quoted in the text and can be >1 in
345 living matter depending on the variable incorporation of excess ^{14}C from nuclear tests^[33],
346 through to 0 when a sample contains no ^{14}C . Surface bulk soil horizons (A-E) from the
347 Central Range Taiwan have an C-weighted average $F_{\text{mod}}=0.98\pm 0.07$ (n=10, ± 1 standard

348 deviation, Supplementary Table 2). We therefore assume that the non-fossil end member
 349 has $F_{\text{mod}}=1$ and fossil $F_{\text{mod}}=0$.

350

351 **POC and suspended sediment transfer.** During typhoon Mindulle POC_{mod} and Q_w
 352 displayed a correlation that can be described by a power law ($\text{POC}_{\text{mod}}=(3.23*10^{-9})$
 353 $*Q_w^{4.03}+1.66$, $R^2=0.99$, $\chi^2=0.6$). With this power law model we obtained a non-fossil
 354 POC transfer of 5500 tC for the full hydrograph of the Mindulle flood from 01/07/2004
 355 07:00 to 12/07/2004 23:00^[31]. For the same period total POC concentration (POC_{tot} , mg
 356 L^{-1}) was related to Q_w ($\text{POC}_{\text{TOT}}=0.30*Q_w^{1.10}$, $R^2=0.87$) and SSC and Q_w were fit by a
 357 power law rating curve ($\text{SSC}=0.76*Q_w^{0.87}$, $R^2=0.93$) giving a total (fossil+non-fossil)
 358 POC transfer of 14,200 tC and a suspended sediment load of 3.88 Mt for the flood.
 359 Combining, the average $C_{\text{org}}*F_{\text{mod}}$ for the flood was 0.14%, a realistic value. With daily
 360 Q_w for 1970-1999, 2003-2004^[31] long term non-fossil POC yields can be estimated, but
 361 samples collected during typhoon Mindulle in 2004 may not represent average
 362 conditions. Indeed, the Mindulle rating curve predicts unrealistic POC_{mod} of 820 g L^{-1} for
 363 the highest Q_w of $3760 \text{ m}^3 \text{ s}^{-1}$ in July 1982. POC_{mod} values in other samples do not lie on
 364 the Mindulle trend (Figure 2). Instead they are described by two power laws that describe
 365 upper and lower bound states related to the supply of non-fossil POC as described in the
 366 main text. Using these power laws ($\text{POC}_{\text{mod}}=0.01*Q_w^{1.59}$, $R^2=0.99$, $\chi^2=1.8$;
 367 $\text{POC}_{\text{mod}}=0.02*Q_w^{1.11}$, $R^2=0.96$, $\chi^2=0.27$) we predict a range of POC_{mod} for a given Q_w and
 368 investigate the long term behavior of the system in the context of the bounds predicted by
 369 these two models.

370 We have three different estimates of the suspended sediment transfer in the LiWu River.
 371 Monthly weighted averaging of Q_w and SSC data from 1970 ($n=553$) gives a sediment
 372 yield of $33,000 \text{ t km}^{-2} \text{ yr}^{-1}$ ^[15]. A rating curve based on our own measurements of SSC and
 373 Q_w in 2004 ($\text{SSC}=55.58*Q_w^{1.17}$, $R^2=0.82$, Supplementary Figure 1, Supplementary Table
 374 1) gives $77,000 \text{ t km}^{-2} \text{ yr}^{-1}$ when applied to the Q_w record since 1970. According to this
 375 rating curve, ~80% of sediment is transferred by floods with a return time of >1/2 year
 376 (Figure 3). However, 2004 SSC data is at the upper end of values measured since 1970
 377 (Supplementary Figure 1), and we consider this yield to be an upper bound. For
 378 comparison, a rating curve based on a least squares best fit of the full gauging record of

379 the Taiwan Water Resources Agency ($SSC=314.37*Q_w^{0.61}$, $R^2=0.33$, Supplementary
380 Figure 1) gives a sediment yield of $13,000 \text{ t km}^{-2} \text{ yr}^{-1}$, which we consider to be a lower
381 bound on the sediment transfer in the LiWu River (Figure 3).

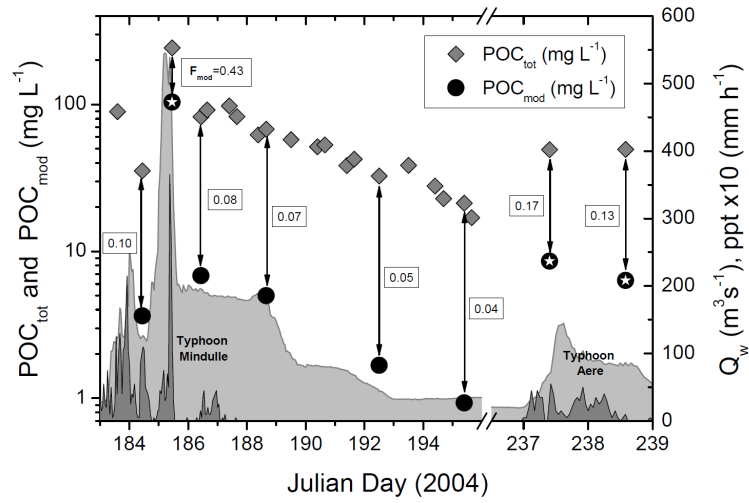
382 31. Data from the Water Resources Agency (WRA), Ministry of Economic Affairs,
383 Taiwan, <http://gweb.wra.gov.tw>, Lushui Gauging Station 2460H005 (2008).

384 32. Gomez, B., Trustrum N. A., Hicks D. M., Rogers K. M., Page M. J., & Tate K. R.
385 Production, storage, and output of particulate organic carbon: Waipaoa River basin, New
386 Zealand. *Water Resour. Res.* **39**, 1161 (2003).

387 33. Levin, I. & Hesshaimer, V. Radiocarbon - A unique tracer of global carbon cycle
388 dynamics. *Radiocarbon* **42**, 69-80 (2000).

389

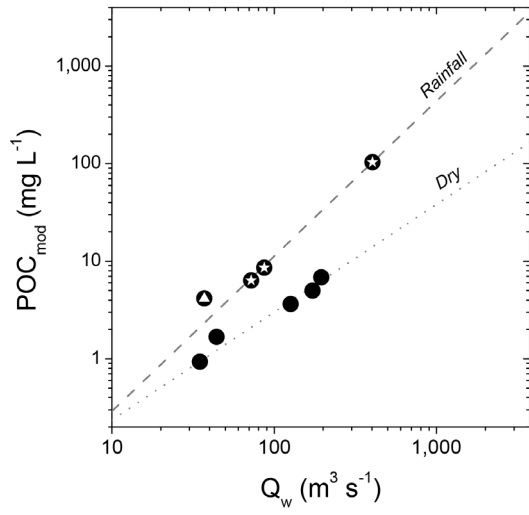
390



391

392 **Figure 1**

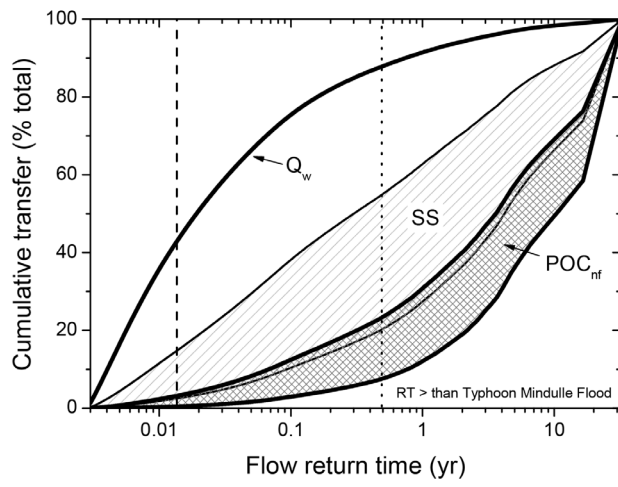
393



394

395 **Figure 2**

396



397

398 **Figure 3**